

Attenuation Properties of DNA Nucleobases Against Nuclear Radiation Using EpiXS, Py-MLBUF, and NGCal Software

G.B. HIREMATH^a, V.P. SINGH^b, P.N. PATIL^{a,c},
N.H. AYACHIT^a AND N.M. BADIGER^{a,*}

^a*School of Advanced Sciences, KLE Technological University, 580031, Hubballi, India*

^b*Department of Physics, Karnatak University, 580003, Dharwad, India*

^c*Radiation Safety and Systems Division, Bhabha Atomic Research Centre, 400085, Mumbai, India*

Received: 23.11.2023 & Accepted: 22.12.2023

Doi: [10.12693/APhysPolA.145.208](https://doi.org/10.12693/APhysPolA.145.208)

*e-mail: nagappa.badiger@kletech.ac.in

In this study, the gamma and neutron interaction parameters of deoxyribonucleic acid and ribonucleic acid nucleobases such as adenine, cytosine, guanine, thymine, and uracil were estimated and compared to those of water. The present calculated mass attenuation coefficient values of deoxyribonucleic acid nucleobases were compared with available simulation code values. From the data, it is observed that guanine has the highest linear attenuation coefficient values among the nucleobases and water in the energy region from 0.015 to 15 MeV. Uracil has a higher effective atomic number and equivalent atomic number values than other nucleobases in the energy region from 0.015 to 15 MeV. Among the nucleobases, uracil has lower buildup factor values, up to 200 keV. However, up to 200 keV, uracil has higher buildup factor values than water. The mass attenuation factor values for nucleobases are listed in the following order: thymine > cytosine > adenine > uracil > guanine. It has been discovered that as the mass attenuation factor increases, the hydrogen wt% of nucleobases also increases.

topics: radiation, DNA, attenuation, buildup factor

1. Introduction

Cancer cells grow abnormally, which leads to the formation of tumors. Radiation kills cancer cells by interacting with DNA (deoxyribonucleic acid) of the cells, where it blocks their ability to divide and proliferate further. High radiation damages the DNA of the cells, both normal and cancerous. Moreover, normal cells usually repair themselves at a faster rate and retain their normal function. Cancer cells, on the other hand, are not as efficient as normal cells. Direct or indirect effects of radiation can damage DNA. In direct action, the radiation would interact with DNA and lead to cell death. Whereas in indirect action, the radiation would create free radicals that damage DNA, leading to cell death. In radiotherapy, radiation is used to kill cancer cells by damaging DNA [1].

Understanding the many characteristics of DNA nucleobases enables the development of a low-cost gene sequencing platform, which has many applications in the fields of medicine, scientific study, and industry [2]. Using low-energy electrons as projectiles, Lampe et al. [3] revealed the mechanistic modeling of DNA damage via Geant4 simulations. Chen et al. [4] investigated radiation damage on an atomistic DNA model using Geant4-DNA toolkit. Tajik et al. [5] used a Monte Carlo

simulation to calculate the direct effects of gamma rays on various DNA structures. Shamshiri et al. [6] studied the direct effect of monoenergetic protons and alpha particles on DNA molecules using Geant4 toolkit. Recently, Al-Buriahi et al. [7] studied the gamma, neutron, and charged particle interaction with DNA nucleobases using the FLUKA code. In the literature, gamma and neutron interaction parameters were studied for glasses [8–10], inorganic compounds [11–14], polymers [15–17], concretes [18], tissue equivalent materials [19–22], biomolecules [23], and alloys [24–26]. So, the authors of this paper have found a gap in the literature where the gamma and neutron interaction parameters were not estimated for DNA and RNA (ribonucleic acid) nucleotides. Therefore, the authors estimated the nuclear radiation interaction parameter for nucleobases.

Therefore, in the present work, the gamma and neutron interaction parameters of DNA and RNA nucleobases such as adenine, cytosine, guanine, uracil, and thymine were studied using EpiXS [27], Py-MLBUF [28], and NGCal [29] software. The gamma ray interaction parameters, such as mass attenuation coefficient (MAC), linear attenuation coefficient (LAC), effective atomic number (Z_{eff}), equivalent atomic number (Z_{eq}), mass-energy absorption coefficient ($M_{en}AC$), effective atomic

Chemical formulae and densities of DNA and RNA nucleobases.

TABLE I

Nucleobases	Chemical formula	Density [g/cm ³]	H	C	N	O
adenine	C ₅ H ₅ N ₅	1.6	0.037296	0.444429	0.518275	–
cytosine	C ₄ H ₅ N ₃ O	1.55	0.045361	0.432426	0.378209	0.144005
guanine	C ₅ H ₅ N ₅ O	2.2	0.033347	0.397379	0.463407	0.105867
thymine	C ₅ H ₆ N ₂ O ₂	1.223	0.047953	0.476193	0.222127	0.253727
uracil	C ₄ H ₄ N ₂ O ₂	1.32	0.035970	0.428627	0.249924	0.285479

number for absorption ($Z_{eff,(en)}$), relative kerma (K_R), exposure buildup factor (EBF), and energy absorption buildup factor (EABF), were estimated using EpiXS [27] and Py-MLBUF [28] software. The neutron interaction parameters, such as mass attenuation factor for thermal and fast neutrons, were estimated using NGCal [29] software. The current estimated values were also compared with those of water in terms of gamma and neutron interaction properties.

2. Theoretical background

Gamma interaction parameters such as MAC, LAC, Z_{eff} , Z_{eq} , EBF, and EABF were estimated using EpiXS [27] software, while $M_{en}AC$, $Z_{eff,(en)}$ and K_R were calculated using Py-MLBUF software [28]. Neutron interaction parameters, such as the mass attenuation factor for thermal and fast neutrons, were estimated using NGCal software [29]. The chemical formula and density of the investigated DNA and RNA nucleobases are shown in Table I. EpiXS software is Windows-based application software that has been constructed for radiation shielding, dosimetry, and photon attenuation and is based on EPDL97 of ENDF/B-VI.8 and EPICS2017 of ENDF/B-VIII. The latest available photoatomic data library is EPICS2017, which is a part of ENDF/B-VIII, and EPDL97 is the photoatomic data library used in Monte Carlo codes such as Geant4, MCNP5, FLUKA, PENELOPE, and PHITS. The Py-MLBUF software is computer code written in Python and hence named Py-MLBUF [28]. It has been developed using a standard database (XCOM, XAAMDI, and ANS standard) verified and validated for elements, compounds, and mixtures against the XCOM code in the energy range of 0.015–15 MeV. FLUKA is a Monte Carlo simulation code used to record the transport of 60 different particles and rays and uses the photoatomic data library of EPDL97. Therefore, it is interesting to compare the EpiXS [27] and FLUKA generated values of MAC to understand how much agreement exists between them. The mass attenuation coefficient for mixture is given by [30–33]

$$\frac{\mu}{\rho} = \sum_i w_i \left(\frac{\mu}{\rho} \right)_i, \quad (1)$$

where μ/ρ represents MAC, and w_i represents the fraction of the weight of element i -th in these samples.

As for effective atomic cross section (σ_a) and total electron cross section (σ_e), they are related to Z_{eff} of the compound or composite material through the relation [30]

$$Z_{eff} = \frac{\sigma_a}{\sigma_e}. \quad (2)$$

The computational work for EBF and EABF was done in three steps, as given below:

- (i) Calculation of the equivalent atomic number, Z_{eq} ;
- (ii) Calculation of the geometrical progression (GP) fitting parameters;
- (iii) Calculation of the exposure and energy absorption buildup factors.

The equivalent atomic number (Z_{eq}) compares the characteristics of composite materials made of equivalent elements to those of a single element's atomic number. Gamma photon interactions with matter are generally known to occur through three processes: photoelectric absorption, Compton scattering, and pair creation. The process of Compton scattering is responsible for the formation of Z_{eq} . However, multiple Compton scattering events primarily contribute to the buildup factor of photons in the material. The values of Z_{eq} can be estimated from the ratio of the Compton mass attenuation coefficient to the total mass attenuation coefficient at the specific photon energy. One should use the relation [30]

$$Z_{eq} = \frac{Z_1 [\log(R_2) - \log(R)] + Z_2 [\log(R) - \log(R_1)]}{\log(R_2) - \log(R_1)}, \quad (3)$$

where Z_1 and Z_2 are the atomic numbers of the elements corresponding to the ratios R_1 and R_2 , respectively. The ratio R is $(\frac{\mu}{\rho})_{Compton}/(\frac{\mu}{\rho})_{total}$ for the selected nucleobases at a specific energy [31].

The equivalent atomic number Z_{eq} is estimated based on the interpolation procedure. Similarly, GP fitting parameters for the selected nucleobases were interpolated using a similar equation, i.e., [30]

$$P = \frac{P_1 [\log(Z_2) - \log(Z_{eq})] + P_2 [\log(Z_{eq}) - \log(Z_1)]}{\log(Z_2) - \log(Z_1)}, \quad (4)$$

TABLE II

Comparison between EpiXS and FLUKA [7] generated MAC values of nucleobases at different photon energy.

Energy [MeV]	EpiXS	FLUKA [7]	Dev. [%]	EpiXS	FLUKA [7]	Dev. [%]	EpiXS	FLUKA [7]	Dev. [%]
	Adenine			Cytosine			Guanine		
0.6	0.08351	0.08357	0.071	0.08417	0.08422	0.059	0.08321	0.08326	0.060
1.25	0.05893	0.05900	0.119	0.05939	0.05946	0.118	0.05872	0.05879	0.119
1.5	0.05362	0.05369	0.130	0.05404	0.05411	0.129	0.05343	0.05350	0.131
2	0.04599	0.04608	0.195	0.04636	0.04644	0.172	0.04584	0.04592	0.174
3	0.03689	0.03697	0.216	0.03719	0.03726	0.188	0.03679	0.03686	0.190
5	0.02806	0.02813	0.249	0.02830	0.02837	0.247	0.02802	0.02809	0.249
10	0.02036	0.02041	0.245	0.02056	0.02061	0.242	0.02041	0.02046	0.244
	Thymine			Uracil			Water		
0.6	0.08438	0.08443	0.059	0.08344	0.08348	0.048	0.08953	0.08956	0.034
1.25	0.05954	0.05961	0.117	0.05887	0.05894	0.119	0.06316	0.06323	0.111
1.5	0.05417	0.05425	0.147	0.05357	0.05364	0.131	0.05747	0.05754	0.122
2	0.04648	0.04656	0.171	0.04597	0.04605	0.174	0.04933	0.04942	0.182
3	0.03729	0.03736	0.187	0.03691	0.03697	0.162	0.03962	0.03969	0.176
5	0.02839	0.02846	0.246	0.02814	0.02821	0.248	0.03024	0.03031	0.231
10	0.02063	0.02069	0.290	0.02054	0.02059	0.243	0.02213	0.02219	0.270

where P_1 and P_2 are the values of GP fitting parameters (b, c, a, X_k, d) corresponding to the atomic numbers Z_1 and Z_2 , respectively, at a specific energy.

Finally, using GP fitting parameters (b, c, a, X_k, d) in the energy range of 0.015–15 MeV up to a penetration depth of 40 mfp, the buildup factors were estimated using the following equations [30, 34–36]

$$B(E, x) = 1 + \frac{b-1}{K-1} (K^x - 1), \quad \text{for } K \neq 1, \quad (5)$$

$$B(E, x) = 1 + (b-1)x, \quad \text{for } K = 1. \quad (6)$$

The function $K(E, x)$ represents the photon dose multiplication factor, which can be calculated using the following equation for $x \leq 40$ mfp

$$K(E, x) = cx^a + d \frac{\tanh\left(\frac{x}{X_k} - 2\right) - \tanh(-2)}{1 - \tanh(-2)}, \quad (7)$$

where b is the accumulation factor at 1 mfp, E is the incident photon energy, and x is the source-to-detector distance for the medium expressed in mean free path [mfp] units. $M_{en}AC$, $Z_{eff,(en)}$, K_R , and MAF were calculated as mentioned elsewhere [37–39].

3. Results and discussion

Figure 1a and b depicts LAC versus photon energy and MAC versus photon energy from 1 keV to 15 MeV, respectively. The LAC values decrease with increasing photon energy, with a slightly sharp fall up at 30 keV. In the lower energy region, the

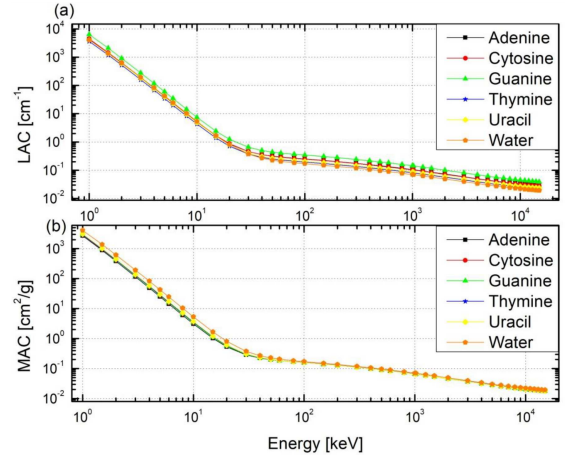


Fig. 1. (a) Linear attenuation coefficient versus energy of X-ray and gamma rays. (b) Mass attenuation coefficient versus energy of X-ray and gamma rays.

photoelectric absorption process is dominant, and as the energy increases further, Compton scattering becomes predominant. The pair production process starts at 1.02 MeV and becomes predominant. As shown in Fig. 1, the LAC values of nucleobases are compared to those of water. Guanine has a higher density, which leads to higher LAC values in the selected energy region. This relationship can be observed in Fig. 1. In lower energy regions, water has higher values of MAC compared to nucleobases because it has a higher content of O. As shown in Table II, the MAC values of nucleobases and water are compared with values generated with

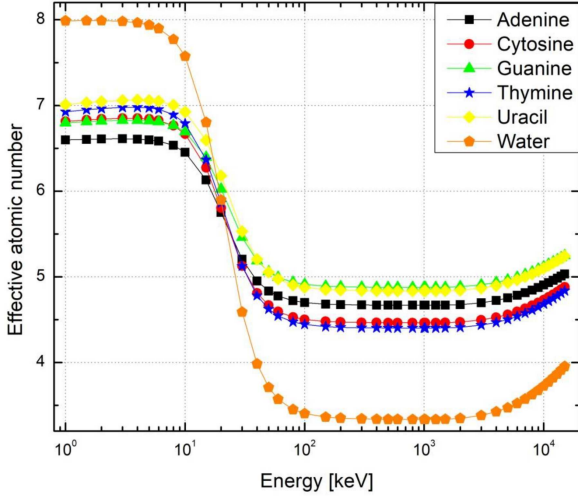


Fig. 2. The effective atomic number as a function of energy of X-rays and gamma rays.

FLUKA code [7] available in the literature. The deviation between the current work results and the FLUKA generated MAC values is 0.3%. First of all, there is a good agreement between them. The current work uses EpiXS software, which uses the latest photoatomic data library, EPICS2017, which has new binding energies and cross-sections [27], whereas FLUKA uses the photoatomic data library, EPDL97. The difference between our MAC values and those generated with FLUKA is due to differences in the photoatomic libraries used by these software tools [10].

Figure 2 depicts Z_{eff} of DNA and RNA nucleobases versus energy in the region from 1 keV to 15 MeV. In the lower energy region, Z_{eff} reaches higher values, as can be noticed in Fig. 2. In the lower energy region, photoelectric absorption predominates and depends upon Z^{4-5} . In the energy range where Compton scattering is dominant, the Z_{eff} values tend to be lower and are influenced by the atomic number (Z). Further, Z_{eff} increases with an increase in the energy of gamma photons. This is due to the pair production process, where it dominates in the higher energy region and depends upon Z^2 . The range of Z_{eff} values for adenine is 6.596–5.032, for cytosine 6.813–4.879, for guanine 6.796–5.248, for thymine 6.925–4.836, for uracil 7.010–5.244, and for water 7.988–3.954, in the energy region from 1 keV to 15 MeV, respectively.

Figure 3 depicts the MenAC values of nucleobases and water as a function of photon energy. It has been observed that MenAC values show a significant decrease in the region of photoelectric absorption, as depicted in Fig. 3. Furthermore, an increase in MenAC values can be observed up to an energy level of 0.6 MeV, followed by a decrease up to 15 MeV, as energy continues to increase. Up to the energy level of 0.1 MeV, the difference between nucleobases and water is from 45% to 9.3%. An increase in energy

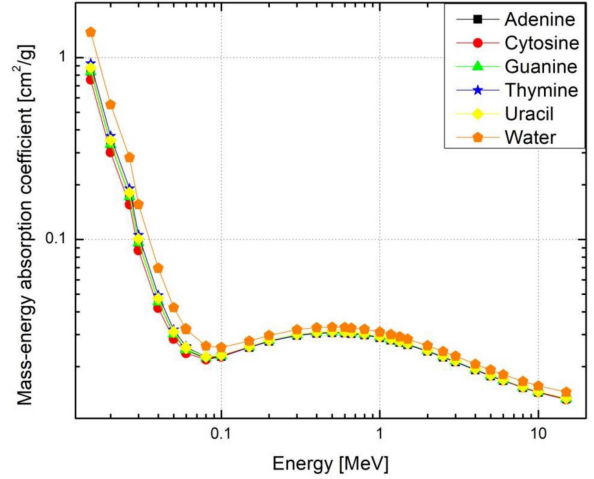


Fig. 3. The mass-energy absorption coefficient as a function of energy of X-rays and gamma rays.

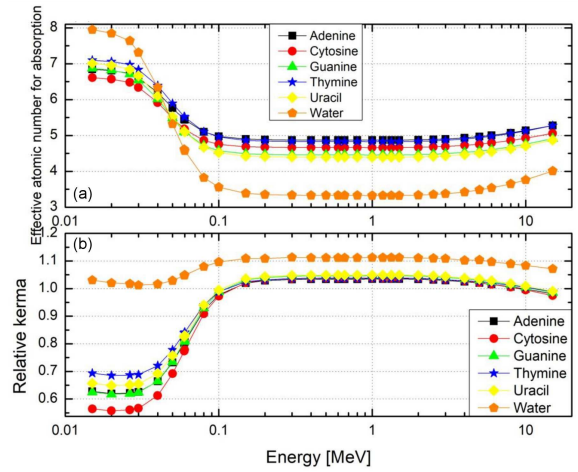


Fig. 4. (a) Effective atomic number for absorption ($Z_{eff,(en)}$) versus the energy of X-ray and gamma rays. (b) Relative kerma as a function of energy of X-ray and gamma rays.

reduces the difference to 5.8%. Figure 4a displays the $Z_{eff,(en)}$ values of nucleobases and water with respect to energy. These values were determined using the Py-MLBUF [28] software and cover the energy range of photons from 0.015 to 15 MeV. As the energy increases up to 0.1 MeV, the value of $Z_{eff,(en)}$ decreases, and the photoelectric absorption becomes the dominant mode of absorption. Compton scattering dominates in the intermediate energy region, and above 1.02 MeV, pair production dominates. As shown in Fig. 4a, $Z_{eff,(en)}$ increases with increasing energy in the pair production region. It is observed that $Z_{eff,(en)}$ depends on the chemical compositions and energy of the photons. The relative kerma K_R of nucleobases and water as a function of energy is shown in Fig. 4b. The K_R values begin to increase as photon energy approaches 0.1 MeV. Further increases are slight and

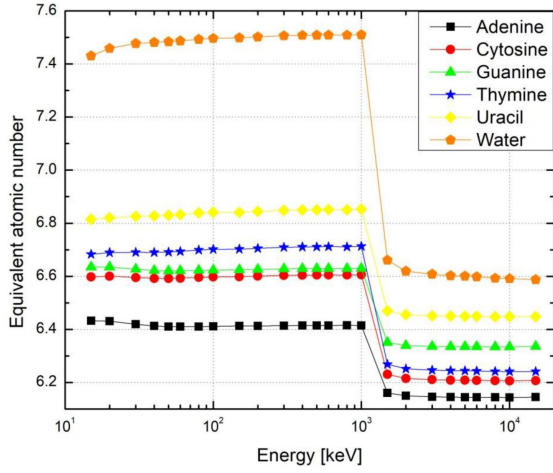


Fig. 5. Equivalent atomic number as a function of energy of X-ray and gamma rays.

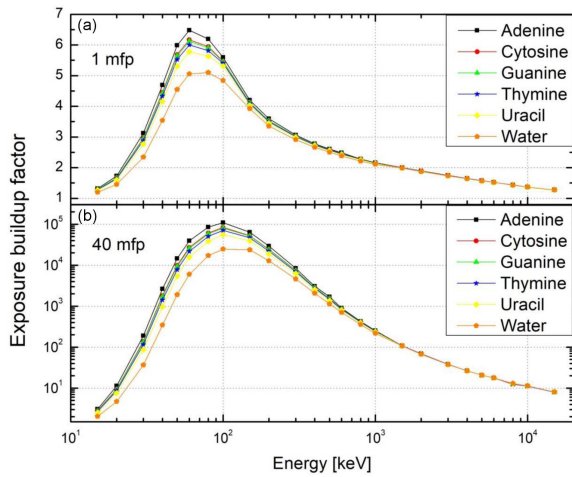


Fig. 6. Exposure buildup factor as a function of energy of gamma photons at selected penetration depth ((a) 1 mfp and (b) 40 mfp).

remain constant up to 2 MeV, and K_R decreases with the decrement in the photon energy, as noticed in Fig. 4b. Water has higher values of K_R compared with nucleobases in the selected energy range of photons from 0.01 to 15 MeV.

In Fig. 5, the energy-dependent Z_{eq} values of water and DNA and RNA nucleobases are presented. It is clearly observed that water has the highest Z_{eq} of the selected photon energy. Also, uracil has higher values of Z_{eq} and adenine has lower values of Z_{eq} among the nucleobases in the photon energy region from 15 keV to 15 MeV. As noticed in Fig. 5, Z_{eq} depends on chemical composition and energy.

Figures 6 and 7 depict EBF and EABF as a function of energy for the investigated DNA and RNA nucleobases and water at 1 mfp and 40 mfp, respectively. Adenine and uracil has higher and lower values of EBF than other investigated nucleobases in the energy region from 30 to 200 keV at 1 mfp and 40 mfp, respectively. Above 1 MeV, the EBF

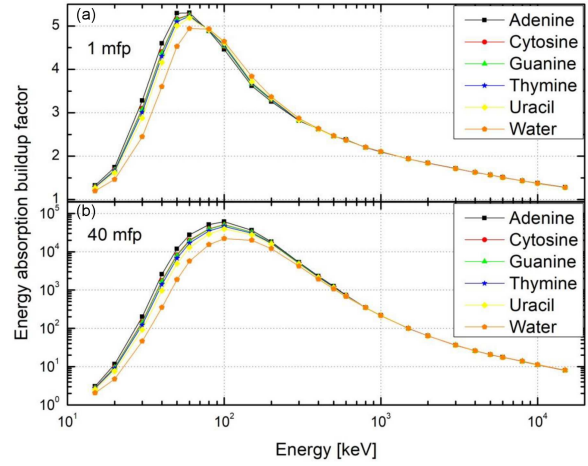


Fig. 7. Energy absorption buildup factor as a function of energy of gamma photons at selected penetration depth ((a) 1 mfp and (b) 40 mfp).

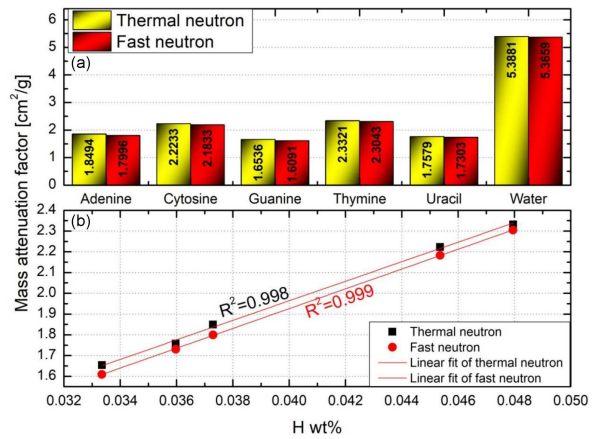


Fig. 8. (a) Mass attenuation factor for thermal and fast neutron versus investigated nucleobases and water. (b) Mass attenuation factor for thermal and fast neutron versus H wt% of investigated nucleobases.

values of nucleobases and water are indistinguishable. Among the investigated nucleobases, adenine and uracil have higher and lower values of EABF in the energy region from 30 to 60 keV at 1 mfp, respectively. However, at 40 mfp, adenine and uracil have higher and lower values of EABF in the energy region from 30 to 200 keV, respectively. The lower EBF and EABF values of uracil compared to other investigated nucleobases are observed, which may be due to its higher content of O than in other nucleobases.

The mass attenuation factor for thermal and fast neutrons was calculated using NGCal [29] software and is shown in Fig. 8a. Among the investigated nucleobases, guanine has lower values of the mass attenuation factor, as observed in Fig. 8a. It may be due to the lower H content in guanine. Mass attenuation factor values for nucleobases are listed

in the following order: thymine > cytosine > adenine > uracil > guanine. Figure 8b depicts the mass attenuation factor versus the weight fraction of H. It is noticed in Fig. 8b that the weight fraction of H for investigated nucleobases increases with an increase in the mass attenuation factor for thermal and fast neutrons.

4. Conclusions

In this study, the gamma and neutron interaction parameters of DNA and RNA nucleobases such as adenine, cytosine, guanine, thymine, and uracil were studied using EpiXS, Py-MLBUF and NG-Cal software. Also, the gamma and neutron radiation interaction parameters of DNA and RNA nucleobases were compared with those of water. The present calculated MAC values of DNA nucleobases were compared with available values generated with FLUKA code. From the data it is observed that guanine has the highest LAC values among nucleobases and water in the energy region from 0.015 to 15 MeV. Uracil has higher Z_{eff} and Z_{eq} values than other nucleobases in the energy region from 0.015 to 15 MeV. Among the nucleobases, uracil has lower buildup factor values up to 200 keV. Moreover, uracil has higher buildup factor values than water, up to 200 keV. Mass attenuation factor values for nucleobases are in following order: thymine > cytosine > adenine > uracil > guanine. It is observed that as the mass attenuation factor increases, the H wt% of nucleobases also increases.

Acknowledgments

N.M.B. thanks the KLE Technological University, Hubballi, India, for funding the capacity building projects and for appointing G.B.H. as a research associate in the project.

References

- [1] R. Baskar, K.A. Lee, R. Yeo, K.-W. Yeoh, *Int. J. Med. Sci.* **9**, 193 (2012).
- [2] E. Mohammadi-Manesh, M. Mir-Mahdevar, *Synth. Met.* **267**, 116486 (2020).
- [3] N. Lampe, M. Karamitros, V. Breton, J.M.C. Brown, I. Kyriakou, D. Sakata, D. Sarramia, S. Incerti, *Phys. Med.* **48**, 135 (2018).
- [4] J. Chen, S. Yun, T. Dong, Z. Ren, X. Zhang, *Nucl. Instrum. Methods Phys. Res. B* **494–495**, 59 (2021).
- [5] M. Tajik, A.S.H. Rozatian, F. Semsarha, *Nucl. Instrum. Methods Phys. Res. B* **346**, 53 (2015).
- [6] P. Shamshiri, G. Forozani, A. Zabihi, *Nucl. Instrum. Methods Phys. Res. B* **454**, 40 (2019).
- [7] M.S. Al-Buriahi, C. Sriwunkum, I. Boukhris, *Eur. Phys. J. Plus* **136**, 776 (2021).
- [8] V.P. Singh, N.M. Badiger, S. Kothan, S. Kaewjaeng, T. Korkut, H.J. Kim, J. Kaewkhao, *Nucl. Sci. Tech.* **27**, 1 (2016).
- [9] V.P. Singh, N.M. Badiger, *Glass Phys. Chem.* **41**, 276 (2015).
- [10] M.B.Z. Gili, J.F.M. Jecong, *Arab. J. Sci. Eng.* (2022).
- [11] M. Dong, S. Zhou, X. Xue, X. Feng, M.I. Sayyed, M.U. Khandaker, D.A. Bradley, *Radiat. Phys. Chem.* **188**, 109601 (2021).
- [12] V.P. Singh, N.M. Badiger, *Vacuum* **113**, 24 (2015).
- [13] Z.Y. Khattari, *J. Aust. Ceram. Soc.* **58**, 521 (2022).
- [14] M.M. Hosamani, A. Vinayak, G.B. Hiremath, P.N. Patil, N.M. Badiger, *Ann. Nucl. Energy* **171**, 109045 (2022).
- [15] P.V. Thulasi, A. Joseph, K.M. Varier, *Radiat. Phys. Chem.* **180**, 109252 (2021).
- [16] M.S. Al-Buriahi, C. Eke, S. Alomairy, A. Yildirim, H.I. Alsaedy, C. Sriwunkum, *Polym. Adv. Technol.* **32**, 2386 (2021).
- [17] C.V. More, H. Alavian, P.P. Pawar, *Appl. Radiat. Isot.* **176**, 109884 (2021).
- [18] V.P. Singh, N.M. Badiger, *J. Ceram.* **2013**, 967264 (2013).
- [19] V.P. Singh, N.M. Badiger, N. Kucuk, *Radioprotection* **49**, 115 (2014).
- [20] I. Kamal, M.K.A. Karim, H.H. Harun, H.R. Abdul Razak, L.Y. Jian, J.L.Y. Chyi, M.M.A. Kechik, *Radiat. Phys. Chem.* **189**, 109661 (2021).
- [21] V.P. Singh, N.M. Badiger, H.R. Vega-Carrillo, *Appl. Radiat. Isot.* **103**, 115 (2015).
- [22] V.P. Singh, N.M. Badiger, *J. Radioanal. Nucl. Chem.* **303**, 1983 (2015).
- [23] M.S. Al-Buriahi, H. Arslan, B.T. Tonguc, *Nucl. Sci. Tech.* **30**, 103 (2019).
- [24] V.P. Singh, N.M. Badiger, *Ann. Nucl. Energy* **64**, 301 (2014).
- [25] A.H. Almuqrin, J.F.M. Jecong, F.C. Hila, C. V Balderas, M.I. Sayyed, *Prog. Nucl. Energy* **137**, 103748 (2021).
- [26] K. Sriwongsa, J. Sirimongkolchaikul, C. Sukrasorn, T. Bussaparoek, S. Kanunghet, T. Phansuea, P. Glumglomchit, P. Limkitjaroenporn, J. Kaewkhao, *Integr. Ferroelectr.* **224**, 120 (2022).

- [27] F.C. Hila, A. Asuncion-Astronomo, C.A.M. Dingle, J.F.M. Jecong, A.M.V. Javier-Hila, M.B.Z. Gili, C.V. Balderas, G.E.P. Lopez, N.R.D. Guillermo, A.V. Amorsolo, *Radiat. Phys. Chem.* **182**, 109331 (2021).
- [28] K.S. Mann, S.S. Mann, *Ann. Nucl. Energy* **150**, 107845 (2021).
- [29] H.S. Gökçe, O. Güngör, H. Yılmaz, *Radiat. Phys. Chem.* **185**, 109519 (2021).
- [30] G.B. Hiremath, M.M. Hosamani, A. Vinayak, P.N. Patil, V.P. Singh, N.H. Ayachit, N.M. Badiger, *Radiat. Eff. Defects Solids* **178**, 335 (2022).
- [31] G.B. Hiremath, M.M. Hosamani, V.P. Singh, N.H. Ayachit, N.M. Badiger, *J. Nucl. Eng. Radiat. Sci.* **9**, 032004 (2023).
- [32] Manjunatha, M.M. Hosamani, G.B. Hiremath, A. Vinayak, V.P. Singh, A.S. Bernal, N.M. Badiger, *Appl. Radiat. Isot.* **201**, 111012 (2023).
- [33] M.M. Hosamani, A. Vinayak, S. Mangeshkar, S. Malode, S. Bhajantri, V. Hegde, G.B. Hiremath, N.M. Badiger, *Spectrosc. Lett.* **53**, 132 (2020).
- [34] K. Hanamar, G.B. Hiremath, B.G. Hegde, N.H. Ayachit, N.M. Badiger, *Optik* **273**, 170397 (2023).
- [35] S.B. Kolavekar, G.B. Hiremath, P.N. Patil, N.M. Badiger, N.H. Ayachit, *Heliyon* **8**, e11788 (2022).
- [36] S.B. Kolavekar, G.B. Hiremath, N.M. Badiger, N.H. Ayachit, *Nucl. Sci. Eng.* **197**, 1506 (2023).
- [37] G.B. Hiremath, V.P. Singh, N.H. Ayachit, N.M. Badiger, *Radiol. Phys. Technol.* **16**, 168 (2023).
- [38] G.B. Hiremath, N.H. Ayachit, N.M. Badiger, *Radiat. Eff. Defects Solids* **178**, 1038 (2023).
- [39] G.B. Hiremath, V.P. Singh, P.N. Patil, N.H. Ayachit, N.M. Badiger, *Radiat. Eff. Defects Solids*, 1 (2023).